

Chapter 3

Structure of the Milky Way

Galactic Astrometry with VLBI

Kazi L. J. Rygl 

INAF-Istituto di Radioastronomia, Via P. Gobetti 101, I-40129 Bologna, Italy.
email: kazi.rygl@inaf.it

Abstract. Astrometric very long baseline interferometry (VLBI) observations of stellar masers are an excellent method to determine distances and proper motions in our Galaxy. Large maser astrometry surveys, the Bar and Spiral Structure Legacy survey and the VLBI Exploration for Radio Astrometry, allowed astronomers to determine fundamental Galactic parameters, such as the rotation curve and the distance to the Galactic centre, as well as to trace the spiral arms. In this review, the results of these surveys will be summarised and compared with astrometric measurements using other methods.

Keywords. Masers, astrometry, VLBI, Milky Way

1. Introduction

Hubble Space Telescope images of nearby, face-on barred spiral galaxies beautifully show their spiral arm structures (Fig. 1). These are traced by bright early-type stars and dark dust lanes. Understanding the spiral structure of our own Galaxy is much harder due to the position of the Sun in the Galactic disk. For us, the Milky Way appears as a starry and dusty lane on the sky (Fig. 2), where at each Galactic longitude we see the emission of the spiral arms in our line of sight, located at different distances from us, superimposed. The high dust extinction in the spiral arms further limits optical wavelengths to detect emission from far away sources. Precise locations of spiral arms in the Galactic plane, their number and structure are therefore much more difficult to measure for the Milky Way than for the nearby face-on galaxies from Fig. 1.

Spectral line Galaxy-wide surveys of HI or CO have the potential to unravel the spiral arm structure in (Galactic) longitude-velocity ($l-v$) diagrams through Galactic rotation patterns. The ($l-v$) diagram of the CO (1–0) line survey of the Galaxy from Dame *et al.* (2001) shows clearly the spiral arms signatures as coherent emission features, whilst the detection of the ellipsoidal brightness distribution at $2.4\ \mu\text{m}$ have shown that the Milky Way is a barred galaxy (Matsumoto *et al.* 1982). However to pinpoint *where* those spiral arms are in three dimensions requires to measure distances on Galactic size scales of about 10 kpc or more at a wavelength that is not obscured by dust.

Using very long baseline astrometry (VLBI) at radio frequencies, which are not affected by dust extinction, astronomers can achieve parallax uncertainties of $10\ \mu\text{arcseconds}$ (e.g., Reid and Honma 2014). Masers around high-mass star-forming regions (HMSFRs) and evolved stars provide bright, point-like targets that can be used for VLBI measurements. In particular, astrometry of HMSFRs, which are known to be located mainly in the spiral arms, is a very powerful method for measuring the structure of the spiral arms and fundamental parameters of our Milky Way, such the Galactic rotation and the distance to the Galactic Centre. In the next sections, I will discuss Galactic astrometry using radio VLBI and specifically radio VLBI of masers, how the two main maser astrometry surveys were conducted, and some of the most important results regarding the Galactic structure obtained by these surveys. After that, I describe the present, new maser survey

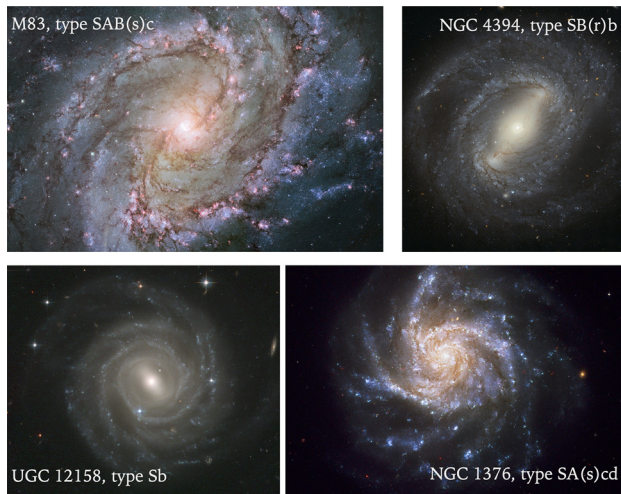


Figure 1. Hubble Space Telescope images of four nearby face-on barred spiral galaxies. Image credits: NASA, ESA, Hubble Heritage Team (STScI/AURA), W. Blair, J. Schmidt and R. Thompson.



Figure 2. The Milky Way as seen from the Atacama Large Millimeter/submillimeter Array site. Image credit: D. Kordan/ESO.

in the Southern hemisphere and improvements on the astrometric accuracy obtained by new calibration methods.

A number of reviews on Galactic maser astrometry with VLBI and comparisons with *Gaia* are readily available, these are Reid and Honma (2014); Xu *et al.* (2018); Immer and Rygl (2022).

2. Astrometry at radio wavelengths using VLBI

2.1. VLBI arrays for astrometry

Table 1 lists the VLBI arrays used for maser astrometry.

In Asia, there is the VLBI Experiment for Astrometry[†] (VERA) array which contains four 20m-antennas located in Japan. Most of the maser astrometry performed with VERA uses the 22 GHz water and SiO masers at ~ 43 GHz, however also 6.7 GHz methanol maser astrometry has been done (Matsumoto *et al.* 2011). The VERA antennas are

[†] The VERA website is available at <https://www.miz.nao.ac.jp/veraserver/index.html>

Table 1. VLBI arrays for maser astrometry.

Array	Max baseline (km)	Angular resolution @6.7 GHz (mas)	Maser species
VERA	2,300	~4	CH ₃ OH, H ₂ O, SiO
VLBA	8,600	~1	OH, CH ₃ OH, H ₂ O, SiO
EVN	10,200	~1	OH, CH ₃ OH, H ₂ O, SiO
LBA	9,800	~1	OH, CH ₃ OH, H ₂ O
ASCI	3,500	~3	CH ₃ OH

equipped with a dual-beam receiver system that permits to observe the maser target and the phase calibrator simultaneously (Honma *et al.* 2008).

The Very Long Baseline Array[†] (VLBA) is a VLBI network in the USA consisting of ten identical 25-m antennas. Its largest baseline is comprised by the station on the Virgin Islands and the station in Hawaii. The VLBA can observe a wide range of masers for astrometry: hydroxyl (OH) around 1.6 GHz; methanol at 6.7 and 12.2 GHz; water at 22 GHz, and the SiO masers both around 43 and 86 GHz. The VLBA was the first VLBI array to perform maser astrometry observations.

The European VLBI Network[‡] (EVN) is a network of (inhomogenous) antennas from Europe, China, Russia, South Africa and Puerto Rico making it the cm VLBI network with the largest baseline separation. Thanks to a number of large dishes, such as the 100m Effelsberg, 65m Tianma and 64m Sardinia Radio Telescope, the EVN is the most sensitive VLBI array on Earth. The EVN can observe all masers from OH masers around 1.6 GHz to SiO masers around 43 GHz. It is the first VLBI network to have measured 6.7 GHz methanol maser parallaxes (Rygl *et al.* 2010). The EVN also observes together with the VLBA, VLA and Green Bank Observatory; these are called global VLBI observations.

In Oceania there are two VLBI arrays, the Long Baseline Array[§] (LBA) and the AuScope-Ceduna-Interferometer (ASCI). These are the only two Southern hemisphere VLBI arrays, which are essential for astrometry in the Galactic Centre region and the fourth Galactic quadrant. The LBA consist of 7 antennas of which 70m Tidbinbilla and 64m Parkes are the largest antennas. The LBA can observe the OH maser around 1.6 GHz, the methanol masers at 6.7 and 12.2 GHz and the 22 GHz water masers. Krishnan *et al.* (2015) performed the first LBA maser astrometry using the 6.7 GHz methanol masers. The ASCI consists of five (inhomogenous) antennas, of which the largest are the 30m Ceduna and the 27m Hobart antennas (Hyland *et al.* 2018). ASCI has receivers in the range of 2.3 - 14 GHz, which include the methanol maser transitions at 6.7 and 12.2 GHz.

2.2. Targets for VLBI astrometry

There are number of compact, non-thermal radio-emitting objects that are interesting for Galactic VLBI astrometry. A few of these are described below.

Non-thermal radio continuum emission in low-mass young stellar objects (YSOs) arises primarily from their magnetosphere. The Goulds Belt Distances Survey (GOBELINS) is a large VLBA programme to measure the parallax and proper motions of YSOs in the nearby star-forming clouds to obtain cloud distances and the 3-dimensional structure of the cloud (e.g., Ortiz-León *et al.* 2017). Toward some of these radio YSOs there is relatively (with respect to high-mass YSOs) little extinction and a comparison between optical *Gaia* and radio astrometry can be made. For example, Ortiz-León *et al.* (2018)

[†] The VLBA website is available at <https://science.nrao.edu/facilities/vlba>

[‡] The EVN website is available at <https://www.evlbi.org/>

[§] The LBA website is available at <https://www.atnf.csiro.au/vlbi/overview/index.html>

have shown there is a good agreement between radio VLBI and *Gaia* astrometry for the YSOs in the Ophiuchos cloud.

PSR π is a large VLBA project to measure radio pulsar distances and proper motions (Deller *et al.* 2016, 2019) which, when combined with their dispersion measures, can help to improve our knowledge of the Galactic electron distribution. The project has obtained parallaxes for 57 pulsars with a median uncertainty of 40 μ as.

Black hole X-ray binaries (BHXBs) are compact radio sources. Black hole formation through a supernova explosion is expected to give these systems a larger natal kick than the direct collapse mechanism. Thus, by measuring the proper motion of BHXBs one try to model the natal kick velocity of that system and learn about the formation of stellar-mass black holes. For example, Atri *et al.* (2019) used VLBI astrometry of the LBA, VLBA and EVN to measure the parallax and proper motion of three BHXB from which they modelled the natal kick velocity distributions.

Maser astrometry and polarization studies can reveal structure, kinematics and magnetic field properties of the masing gas on tens to thousands au-scales around YSOs as shown by Sanna *et al.* (2010, 2015) for HMSFR G023.01-00.41. Recently Moscadelli *et al.* (2022, 2023) used global VLBI observations of 22 GHz water masers to provide the first observational evidence of a disk wind in the high-mass YSO IRAS 21078+5211. Maser astrometry can also be used to study the structure of star-forming complexes. For example, Rygl *et al.* (2012) measured maser astrometry towards five HMSFRs toward the Cygnus X region, determining the membership of the Cygnus X complex, its distance and its structure and velocity distribution. On larger scales, using a number of HMSFRs maser astrometry can reveal the structure and kinematics of spiral arms. Sakai *et al.* (2019) found that HMSFRs in the inner part of the Perseus spiral arm have a significant radial inward motion which agrees with models of star-formation through gas shocks when encountering the slower-rotation spiral arm (Roberts 1969, 1972). Zooming out even more, to Galactic scales, one can use maser astrometry to measure the spiral arm positions and determine fundamental parameters of the Milky Way as discussed in the next sections.

3. Measuring Galactic structure through maser VLBI astrometry

High-mass (OB-type) stars form in dense, molecular clouds that commonly found in the spiral arms. Figure 1 shows how the spiral arms are the locations of extinction, the ‘dark lanes’ and the bright OB-type stars (for an overview of spiral arm tracers see Xu *et al.* 2018). Time scales for high-mass star formation are of the order of 10^5 years or less (see Motte *et al.* 2018, and references therein) and lifetimes of OB type stars are of the order of few 10^5 years (Weidner and Vink 2010). These very short lifetimes imply that these objects could not have moved far from their birth sites and are likely still carrying the kinematic imprint of the gas from which they formed. This is why HMSFRs and OB-type stars are excellent tracers of spiral arm structure and Galactic rotation. The advantage of VLBI maser astrometry of HMSFRs is the lack of extinction at radio wavelengths combined with milliarcsecond angular resolution that allows astronomers to measure parallaxes and proper motions out to even 20 kpc (Sanna *et al.* 2017).

3.1. Masers in high-mass star-forming regions and evolved stars

The most common masers found towards HMSFRs are the 22 GHz water masers, which may be located in the disk around the YSO, in the envelope, in the disk-wind, but also in the outflows, as is the case for the water masers in the Turner-Welch object in W3 (Hachisuka *et al.* 2015). For methanol masers two transitions, at 6.7 and 12.2 GHz, are used for astrometry. These maser species are more often found in the disk or envelope

around the YSO. Bartkiewicz *et al.* (2020) found that the 6.7 GHz methanol masers in high-mass YSO G23.657-00.127 are expanding, and are likely tracing a spherical outflow or a wide-angle wind at the base of the proto-stellar jet. Most methanol astrometry studies use the 6.7 GHz transition because it is brighter, ubiquitous, and so far found exclusively in HMSFRs Menten (1991). A few SFRs may also exhibit SiO masers in their outflows; for example, Kim *et al.* (2008) used 43 GHz SiO masers in Source I to derive a parallax to Orion. Their result was in excellent agreement with the parallax of non-thermal emission of low-mass stars in Orion from Menten *et al.* (2007) and Sandstrom *et al.* (2007).

Evolved star envelopes are rich in maser emission (see Matthews 2023). They mainly emit in 1.6 GHz OH, 22 GHz water and 43 (and 86) GHz SiO masers. For example, Matsuno *et al.* (2020) performed astrometric 22 GHz water maser observations of the asymptotic giant branch (AGB) star BX Cam. In addition to the parallax and proper motions, they measured that the maser features have an expansion velocity of about 15 km s^{-1} . The evolved stars with maser emission are typically AGB stars or red super giants (RSGs). RSGs evolve from high-mass stars and have a lifetime of \sim tens of Myr. AGB stars evolve from low-mass stars and have therefore much larger ages. This implies that both these kinds of evolved stars, but especially the AGB stars, are not very good tracers of spiral structure as they have moved away from their natal sites. However, on the contrary to the high extinction towards HMSFRs which makes any optical measurements impossible, many evolved stars have optical parallaxes measured by *Gaia* and a comparison between radio and optical astrometry is possible. In particular, for the validation of the *Gaia* reference frame of bright stars Lindegren (2020) compared the *Gaia* astrometry with VLBI astrometry of continuum emitting of low-mass YSOs and masing evolved stars.

3.2. Large astrometric surveys

Recently two large VLBI maser parallax programmes have published their collective results. The two programmes are the Bar and Spiral Structure Legacy (BeSSeL) survey (Brunthaler *et al.* 2011; Reid *et al.* 2019) and the VERA collaboration (VERA Collaboration *et al.* 2020; Honma 2023).

The BeSSeL survey is a key science project of the VLBA and used 6.7 and 12.2 GHz methanol and 22 GHz water masers. The VERA survey used 22 GHz water and SiO masers around 43 GHz.

3.3. Parallax and proper motions from relative astrometry

Both BeSSeL and VERA surveys measure relative positions of the maser spots with respect to one or more position reference sources (compact quasars) over the course of one year. This allows to measure and separate the sinusoidal parallax signature and the linear proper motion of the target in each coordinate.

The number of epochs used for astrometric observations depends mainly on the maser species. The less variable methanol masers were observed in four epochs, sampling the minima and maxima of the Right Ascension parallax signal. Water masers, which are more variable have typically 6 epochs spread over one year in the BeSSeL survey, but sometimes more epochs over a longer duration were observed. VERA water maser and SiO astrometry typically observed every one or two months for a year, but some targets were tracked for more than 2 years.

Both these surveys rely on phase referencing observations, where the atmospheric delay is calibrated on a nearby position reference source (typically a quasar) that is assumed to have the same delay as the target. This method allows to achieve tens of microarcsecond *relative* position accuracy over baselines of 8,000 km for a 1° separation between target

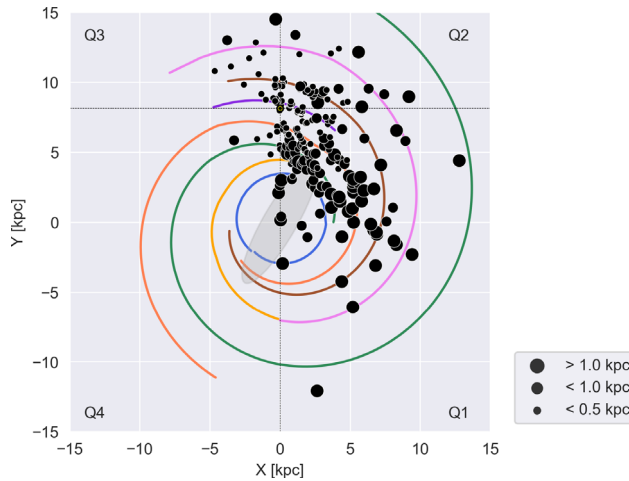


Figure 3. HMSFR distribution in the Milky Way based on maser parallaxes, shown in a plan-view of the Milky Way seen from the north Galactic pole. Data used are from [Reid *et al.* \(2019\)](#); [VERA Collaboration *et al.* \(2020\)](#); [Xu *et al.* \(2021\)](#); [Hyland *et al.* \(2022b\)](#), and references therein. Adapted figure from [Immer and Rygl \(2022\)](#).

and position reference source. This is the accuracy required to reach the ~ 10 microarc-second parallax uncertainties necessary for Galactic-scale distances. In the case of maser astrometry, inverse-phase referencing is done, calibrating on a bright maser spot as these have a much higher signal-to-noise ratio than the position reference sources. More details can be found in the review by [Reid and Honma \(2014\)](#).

4. Structure and fundamental parameters of our Milky Way: results from maser astrometry

Figure 3 shows a plan-view of the Milky Way with the positions of 233 HMSFRs and RSG with maser parallax astrometry taken from [Reid *et al.* \(2019\)](#); [VERA Collaboration *et al.* \(2020\)](#); [Xu *et al.* \(2021\)](#); [Hyland *et al.* \(2022b\)](#). Around the Sun's position in the plane, the Milky Way is divided in four quadrants. It is clear that the first and second quadrants are rather well covered by the maser astrometry surveys, the third only in part and the fourth hardly. The more filled quadrants correspond to the part of the sky that can be observed well from the Northern Hemisphere where most of the VLBI arrays, that have been used for maser astrometry up to now, are located.

Furthermore, there are notably few targets on the far side of the Galaxy (beyond the Galactic Centre), in the Galactic Centre region and in the outer regions of the Milky Way (at large Galactocentric radii). It is more difficult to measure smaller parallax signatures, and Fig. 3 also shows that the farther targets have typically larger uncertainties. The other reason is the scarceness of maser astrometry targets where there is fewer star formation activity. The Galactic Centre region has a lower star formation rate than the disk and thus fewer maser targets ([Barnes *et al.* 2017](#)). Any new maser astrometry result in this region is very important for our understanding of the structure and dynamics of the Galactic bar, see also [Kumar *et al.* \(2023\)](#). At large Galactocentric radii the star formation activity is notably less than in the inner Galaxy. This is visible in Fig. 3 by fewer astrometric data available for these regions.

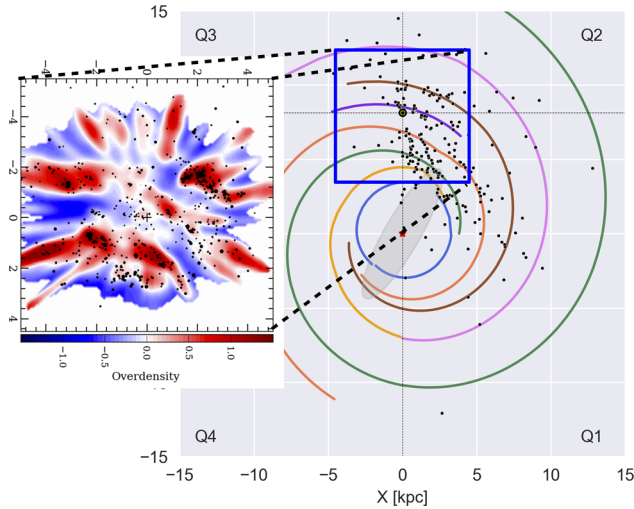


Figure 4. Same as Figure 3, but now showing the area for which *Gaia* DR3 astrometry of OB-type stars is available. The inset shows the over density of the OB-type stars from [Gaia Collaboration et al. \(2022a\)](#) rotated to follow the same orientation as the underlying figure.

4.1. Spiral arm structure

Combining the parallax and proper motions with the sky positions and a local-standard-of-rest (LSR) velocity, one can obtain a 3-dimensional position and velocity data point for each maser astrometry target.

To derive the spiral arm structure, [Reid et al. \(2019\)](#) assigned spiral arm membership to each maser astrometry target as follows. Where possible, spiral arm designations were assigned by associating their Galactic longitude and LSR velocity to molecular clouds of a spiral arm in the $(l-v)$ diagram of CO or HI data ([Weaver 1974](#); [Cohen et al. 1980](#); [Dame et al. 2001](#)). For objects with unclear arm associations through this method, also their parallax, proper motion, and Galactic latitude were used through the Bayesian distance calculator ([Reid et al. 2016, 2019](#)) to find the best matching spiral arm.

[Reid et al. \(2019\)](#) then fitted log-periodic spirals to HMSFRs with spiral arm memberships to derive the parameters for the spiral arms. These derived spiral arm models are shown in color in Figures 3, 4.

Other tracers of spiral arms are OB-type stars for which the *Gaia* satellite can measure parallaxes and proper motions. Due to the dust extinction in the Galactic plane, the latest *Gaia* DR3 data have still a rather limited range of ~ 3 kpc distance from the Sun where their parallax uncertainties are 10% or better. Nevertheless, within this range, Fig. 4 shows that the OB-type star traced arms [Gaia Collaboration et al. \(2022a\)](#) match well with those from maser VLBI astrometry, as expected.

4.2. Galactic rotation curve

The motion of each maser astrometry target is a combination of its Galactic rotation at its Galactocentric radius, its peculiar motion, and the Solar motion. Therefore, Galactic rotation curves can be fitted to the three dimensional space velocities of a large number of HMSFRs (and a few super giants) spread over the Galactic plane (as shown in Fig. 3). Both the BeSSeL and the VERA teams used Bayesian Markov Monte Carlo Chain fitting routines, but with different parametrisations of the Galactic rotation curve, a (slightly)

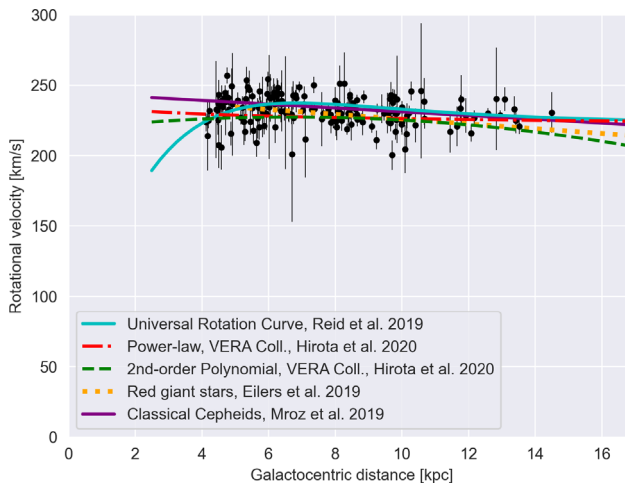


Figure 5. Galactic rotation curves from VLBI maser astrometry (Reid *et al.* 2019; VERA Collaboration *et al.* 2020), from RGSs (Eilers *et al.* 2019) and Classical Cepheids (Mróz *et al.* 2019). The rotational velocity of maser sources (Reid *et al.* 2019; VERA Collaboration *et al.* 2020) is shown by black dots. Figure taken from Immer and Rygl (2022).

different number of maser targets and different priors (for example the Solar motion prior). Details of the fitting can be found in Reid *et al.* (2019) for the BeSSeL survey and in VERA Collaboration *et al.* (2020) for the VERA survey.

In Figure 5, the rotation curves derived by maser astrometry (Reid *et al.* 2019; VERA Collaboration *et al.* 2020) are shown and compared to those from RGSs (Eilers *et al.* 2019) and classical Cepheids (Mróz *et al.* 2019). The maser-based rotation curves were derived from data at Galactocentric radii ≥ 4 kpc since the motions in the inner Galaxy are expected to be influenced by the Galactic bar. While the shape of each of these curves is a bit different, within the region covered by maser data (from 4 to almost 15 kpc, but getting scarcer with larger radii) the rotation curves are quite similar and nearly flat. Note that the RGSs and classical Cepheids rotation curves are derived from Galactocentric radii out to 20 or even 25 kpc. Nevertheless, they agree rather well with the maser-based rotation curves. Figure 5 shows that the rotational velocity is expected to decrease slowly with radius for all curves. However, the RGSs curve (Eilers *et al.* 2019) is decaying faster than that of the classical Cepheids (Mróz *et al.* 2019). To investigate this decrease with maser astrometry more data in the outer Galaxy are needed. Unfortunately, the star-formation activity in the Outer spiral arm is rather low, and finding HMSFRs with bright enough masers for astrometry is not an easy task.

4.3. Distance to the Galactic Centre

By fitting the Galactic rotation curve to maser astrometry data also a distance to the Galactic Centre (R_0) is obtained. Figure 6 shows on the top the two measurements from maser astrometry: $R_0 = 8.15 \pm 0.15$ kpc (Reid *et al.* 2019) and $R_0 = 7.92 \pm 0.16_{\text{stat}} \pm 0.3_{\text{sys}}$ kpc (VERA Collaboration *et al.* 2020). These two measurements agree well within their uncertainties. It is interesting to see how good these measurements agree with Galactic distances from other methods. The maser astrometry values agree well with the R_0 measurements from other methods as shown in Fig. 6: kinematics of Galactic bar stars (8.23 ± 0.12 kpc, Leung *et al.* 2023), radial velocities of stars (8.27 ± 0.29 kpc, Schönrich 2012), *Gaia* DR2 astrometry of OB-type stars

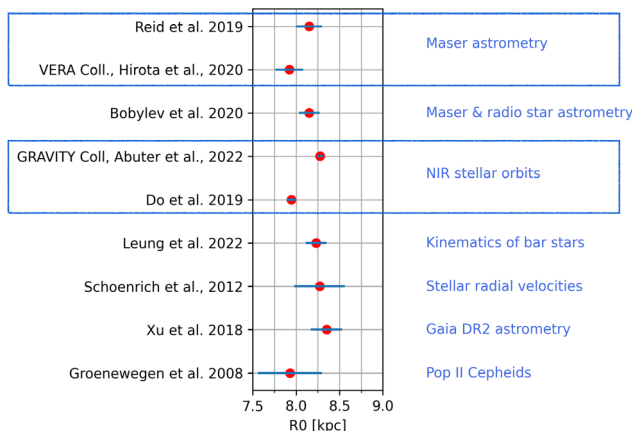


Figure 6. Distance to the Galactic Centre (R_0) as measured by various methods.

(8.35 ± 0.18 kpc, [Xu et al. 2018](#)), maser and radio star astrometry ($8.15^{+0.04}_{-0.20}$ kpc, [Bobylyev et al. 2020](#)) and Pop II Cepheids (7.93 ± 0.37 kpc, [Groenewegen et al. 2008](#)). Above all, the two most precise measurements of R_0 , based on the measurements of stellar orbits around the Galactic Centre supermassive black hole, obtained $R_0 = 7.946 \pm 0.050_{\text{stat}} \pm 0.032_{\text{sys}}$ kpc using adaptive optics techniques with the Keck telescope ([Do et al. 2019](#)), and $8.277 \pm 0.009_{\text{stat}} \pm 0.033_{\text{sys}}$ kpc with the Very Large Telescope Interferometer ([Gravity Collaboration et al. 2022](#)). While these values are in a slight tension with each other, both of them agree well with the maser astrometry values, which have larger uncertainties.

4.4. Sgr A* as the dynamic centre of the Milky Way

The full angular velocity of the Sun, Ω_{\odot} , obtained from maser astrometry is $\Omega_{\odot} = 30.32 \pm 0.27$ km s $^{-1}$ kpc $^{-1}$ ([Reid et al. 2019](#)) and $\Omega_{\odot} = 30.17 \pm 0.27$ km s $^{-1}$ kpc $^{-1}$ ([VERA Collaboration et al. 2020](#)). These two values, which are in good agreement with each other, can then be compared to the apparent proper motion of Sgr A* in the direction of Galactic longitude, -6.411 ± 0.008 mas yr $^{-1}$, measured by [Reid and Brunthaler \(2020\)](#). Assuming that Sgr A* is stationary, this motion can be interpreted as the reflex motion of the Sun in the direction of Galactic rotation. This would yield 30.39 ± 0.04 km s $^{-1}$ kpc $^{-1}$ as angular velocity at the Sun, which is indeed in excellent agreement.

This agreement underlines the validity of the assumption of Sgr A* being stationary in the rotating Galactic disk, making it the dynamic centre of the Milky Way. Notably, Galactic-wide velocity fields mapped by HMSFRs over ~ 10 kpc radii and the stellar orbits at 1000s au around Sgr A* yield a consistent distance to the Galactic Centre.

4.5. Galactic mid plane and warp

[Reid et al. \(2019\)](#) have shown that HMSFRs with Galacto-centric distances ≤ 7 kpc, thus not affected by the Galactic warp, have a very narrow distribution in Galactic latitude. The peak of their distribution is at negative Galactic latitudes and not at 0° which would be expected if the Sun would be in the midplane of the disk. These authors used the latitude distribution of maser-bearing HMSFRs to derive the height of the Sun with respect to the midplane finding $Z_{\odot} = 5.5 \pm 5.8$ pc. Using this value to correct the IAU Z-plane, shifts the position of Sgr A* (which has $Z_{\text{IAU}} = -6.5$ pc when using

d=8.15 kpc) into to the Galactic midplane where one would expect it to be if Sgr A* is our dynamical centre.

In the outer parts of the Milky Way, maser astrometry can be used to trace the Galactic warp. Sakai *et al.* (2020) performed maser astrometry of Outer arm sources in the second quadrant. They found that between Galactic azimuth[†] of 20 and 50 degrees the scale height of the HMSFRs increases in a sinusoidal wave fashion from Galactocentric distances of 10 kpc onwards reaching heights above the midplane of $Z=200\text{--}600$ pc. In addition to positions, Sakai *et al.* (2020) also investigated the W-motion (in direction of the north Galactic pole) finding it could be fitted well with a sinusoidal curve of about 10 km s^{-1} which reaches 0 km s^{-1} at the Galactocentric radius with the highest Z . This wave-like distribution is also seen in the classical Cepheids distribution of Skowron *et al.* (2019) in that part of the Milky Way. Classical Cepheids with their ages of ≤ 400 Myr are considered still relatively good tracers of the Galactic disk. The advantage of Cepheid studies is that there are many more Cepheid stars available and that these reach out to larger Galactocentric radii than maser-bearing stars.

4.6. High proper motions in the Scutum arm: evidence of the Galactic bar?

Aside of measuring locations and Galactic rotation velocity components, one obtains the three-dimensional peculiar motions of the maser-bearing SFR. When measuring the parallaxes and proper motions of the Scutum spiral arm, Immer *et al.* (2019) found that there were a number of HMSFRs in this spiral arm, at azimuths where the arm is in the vicinity of the tip of the Galactic bar, that showed exceptionally large ($> 20\text{ km s}^{-1}$) peculiar motions. The authors put forward a combined gravitational attraction of the Galactic bar and the spiral arm potential as the most likely explanation. This fascinating kinematic signature of star-forming gas near the tip of the Galactic Bar was modelled by Li *et al.* (2022) using hydrodynamical simulations of gas in a Milky-Way-like barred spiral galaxy. These simulations reproduced very well the velocity field at the positions of the HMSFRs. In the residual (after subtraction the Galactic rotation) radial velocity component of the gas, the rotation of the gas around the Galactic bar is very evident. *Gaia* astrometry of RGB stars found the same distribution in radial velocities as in the simulations. The combination of maser and stellar astrometry with simulations testify to the strong influence of the Galactic bar on the dynamics of the Milky Way.

5. The future: next generation large projects, new calibration techniques and better comparisons with *Gaia*

5.1. Southern hemisphere VLBI maser astrometry

Figure 3 shows the VLBI maser astrometry coverage of the Galactic plane with the rather empty fourth and third quadrants. Southern Hemisphere VLBI maser astrometry is necessary to study this part of the Milky Way, and also the Galactic Centre which is particularly interesting because of the bar. The new, Southern Hemisphere Parallax Interferometric Radio Astrometry Legacy Survey (S π RALS) is a 6.7 GHz methanol maser astrometry survey using the ASCI array. Hyland *et al.* (2022b) published the first astrometric results of this survey, showing to be able to obtain consistent results for HMSFR G232.62+00.99 to those from 12.2 methanol maser astrometry (Reid *et al.* 2009) and delivering maser astrometry for one new target (see also Hyland *et al.* 2023). Furthermore, Kumar *et al.* (2023) have been using ASCI 6.7 GHz data of the Galactic Centre region to study the structure and dynamics of the bar. To improve the Galactic parameters

[†] Galactic azimuth has the origin in the Galactic Centre and is defined as having zero degree in the direction to the Sun, increasing clock-wise.

derived from maser astrometry, it is crucial to have a good coverage the Galactic velocity field, so results of the S π RALS project are eagerly awaited.

5.2. New phase referencing techniques

When doing 6.7 GHz methanol maser astrometry, it was noted that uncompensated dispersive delays due to the ionosphere can cause positional shifts. Reid *et al.* (2017); Wu *et al.* (2019) then devised an approach to estimate and correct for these position shifts, following the MultiView method (Rioja *et al.* 2017; Rioja 2023) but in the image plane. To improve the ionospheric calibration, the S π RALS observations use the MultiView method (Rioja *et al.* 2017), that employs multiple position reference sources at different position angles of the maser target to interpolate the ionospheric delay at the target position. In fact, as the bright maser emission is used for phase-referencing, this method is called inverse MultiView. Hyland *et al.* (2022a) showed that for their two HMSFRs their parallax uncertainties using inverse MultiView were around 10 microarcseconds while when using inverse phase referencing to the various position reference sources the uncertainties were much bigger (in the range of 25 to 60 microarcseconds) and increasing with the separation between the maser and position reference target. A review of the technical improvements including the MultiView technique is discussed in Rioja and Dodson (2020).

5.3. Gaia comparisons with maser astrometry

In the latest DR3, *Gaia* has released the astrometry of almost 1.5 billion stars (Gaia Collaboration *et al.* 2022b; Jordi *et al.* 2023). For the AGB star, BX Cam, discussed earlier in Section 3.1, Matsuno *et al.* (2020) measured a 22 GHz water maser parallax of 1.73 ± 0.03 mas. The DR2 *Gaia* parallax of this star, 4.134 ± 0.25 mas, was quite problematic. However, with the improved astrometric accuracy of DR3 the newest *Gaia* DR3 parallax of 1.764 ± 0.10 mas for BX Cam is in very good agreement. This opens up many venues of interesting comparisons between VLBI maser astrometry and optical *Gaia* astrometry for stellar maser targets.

6. Summary

The large VLBI maser astrometry surveys BeSSeL and VERA have measured astrometry to more than 200 HMSFRs and evolved stars. With these data spiral arms have been traced in the Galactic plane. The measured 3-D velocity field of these maser stars permitted an accurate determination of the distance to the Galactic centre and the Galactic rotation. Evidence of the Galactic warp, both in position and velocity, has been measured from maser parallaxes. In the inner Galaxy, the peculiar velocities of HMSFRs are a testimony to the large influence of the bar on Galactic dynamics. With the new maser astrometric survey S π RALS in the Southern Hemisphere exciting new astrometric results will map out the uncharted territory in the forth and third quadrant of Milky Way, which will allow astronomers to improve determination of the Galactic parameters in the future.

References

- Atri, P., Miller-Jones, J. C. A., Bahramian, A., *et al.* 2019, *MNRAS*, 489(3), 3116
- Barnes, A. T., Longmore, S. N., Battersby, C., *et al.* 2017, *MNRAS*, 469(2), 2263
- Bartkiewicz, A., Sanna, A., Szymczak, M., Moscadelli, L., *et al.* 2020, *A&A*, 637, A15
- Bobylev, V. V., Krisanova, O. I., & Bajkova, A. T. 2020, *Astronomy Letters*, 46(7), 439
- Brunthaler, A., Reid, M. J., Menten, K. M., *et al.* 2011, *Astronomische Nachrichten*, 332(5), 461
- Cohen, R. S., Cong, H., Dame, T. M., & Thaddeus, P. 1980, *ApJ*, 239, L53

- Dame, T. M., Hartmann, D., & Thaddeus, P. 2001, *ApJ*, 547(2), 792
- Deller, A. T., Goss, W. M., Briskin, W. F., *et al.* 2019, *ApJ*, 875(2), 100
- Deller, A. T., Vigeland, S. J., Kaplan, D. L., *et al.* 2016, *ApJ*, 828(1), 8
- Do, T., Hees, A., Ghez, A., *et al.* 2019, *Science*, 365(6454), 664
- Eilers, A.-C., Hogg, D. W., Rix, H.-W., & Ness, M. K. 2019, *ApJ*, 871(1), 120
- Gaia Collaboration, Drimmel, R., Romero-Gomez, M., Chemin, L., *et al.* 2022a, *A&A*, 674, A37
- Gaia Collaboration, Vallenari, A., Brown, A. G. A., Prusti, T., *et al.* 2022b, *A&A*, 674, A1
- Gravity Collaboration, Abuter, R., Aimar, N., Amorim, A., *et al.* 2022, *A&A*, 657, L12
- Groenewegen, M. A. T., Udalski, A., & Bono, G. 2008, *A&A*, 481(2), 441
- Hachisuka, K., Choi, Y. K., Reid, M. J., *et al.* 2015, *ApJ*, 800(1), 2
- Honma, M., Kijima, M., Suda, H., *et al.* 2008, *PASJ*, 60(5), 935
- Honma, M. 2023, in this volume
- Hyland, L. J., Ellingsen, S. P., & Reid, M. J. 2018, in A. Tarchi, M. J. Reid, M. J. & P. Castangia (eds.), *Astrophysical Masers: Unlocking the Mysteries of the Universe*, Proc. IAU Symposium, 336, p. 154
- Hyland, L. J., Reid, M. J., Ellingsen, S. P., *et al.* 2022a, *ApJ*, 932 (1), 52
- Hyland, L. J., Reid, M. J., Orosz, G., *et al.* 2022b, *ApJ*, 953(1), 21
- Hyland, L. J., *et al.* 2023, in this volume
- Immer, K., Li, J., Quiroga-Núñez, L. H., *et al.* 2019, *A&A*, 632, A123
- Immer, K. & Rygl, K. L. J. 2022, *Universe*, 8(8), 390
- Jordi, C., *et al.* 2023, in this volume
- Kim, M. K., Hirota, T., Honma, M., *et al.* 2008, *PASJ*, 60, 991
- Krishnan, V., Ellingsen, S. P., Reid, M. J., *et al.* 2015, *ApJ*, 805(2), 129
- Kumar, J., *et al.* 2023, in this volume
- Leung, H. W., Bovy, J., Mackereth, J. T., *et al.* 2023, *MNRAS*, 519(1), 948
- Li, Z., Shen, J., Gerhard, O., & Clarke, J. P. 2022, *ApJ*, 925(1), 71
- Lindgren, L. 2020, *A&A*, 633, A1
- Matthews, L. 2023, in this volume
- Matsumoto, N., Honma, M., Isono, Y., *et al.* 2011, *PASJ*, 63, 1345
- Matsumoto, T., Hayakawa, S., Koizumi, H., *et al.* 1982, in G. R. Riegler & R. D. Blandford (eds.), *The Galactic Center*, AIP Conference Series, 83, p. 48
- Matsuno, M., Nakagawa, A., Morita, A., *et al.* 2020, *PASJ*, 72(4), 56
- Menten, K. M. 1991, *ApJ*, 380, L75
- Menten, K. M., Reid, M. J., Forbrich, J., & Brunthaler, A. 2007, *A&A*, 474(2), 515
- Moscadelli, L., Sanna, A., Beuther, H., Oliva, A., & Kuiper, R. 2022, *Nature Astronomy*, 6, 1068
- Moscadelli, L., *et al.* 2023, in this volume
- Motte, F., Bontemps, S., & Louvet, F. 2018, *ARA&A*, 56, 41
- Mróz, P., Udalski, A., Skowron, D. M., *et al.* 2019, *ApJ*, 870(1), L10
- Ortiz-León, G. N., Loinard, L., Dzib, S. A., *et al.* 2018, *ApJ*, 865(1), 73
- Ortiz-León, G. N., Loinard, L., Kounkel, M. A., *et al.* 2017, *ApJ*, 834(2), 141
- Reid, M. J. & Brunthaler, A. 2020, *ApJ*, 892(1), 39
- Reid, M. J., Brunthaler, A., Menten, K. M., *et al.* 2017, *AJ*, 154(2), 63
- Reid, M. J., Dame, T. M., Menten, K. M., & Brunthaler, A. 2016, *ApJ*, 823(2), 77
- Reid, M. J. & Honma, M. 2014, *ARA&A*, 52, 339
- Reid, M. J., Menten, K. M., Brunthaler, A., *et al.* 2019, *ApJ*, 885(2), 131
- Reid, M. J., Menten, K. M., Brunthaler, A., *et al.* 2009, *ApJ*, 693(1), 397
- Rioja, M. J., Dodson, R., Orosz, G., Imai, H., & Frey, S. 2017, *AJ*, 153(3), 105
- Rioja, M. J. & Dodson, R. 2020, *A&A Rev.*, 28(1), 6
- Rioja, M. J. 2023, in this volume
- Roberts, W. W. 1972, *ApJ*, 173, 259
- Roberts, W. W. 1969, *ApJ*, 158, 123
- Rygl, K. L. J., Brunthaler, A., Reid, M. J., *et al.* 2010, *A&A*, 511, A2
- Rygl, K. L. J., Brunthaler, A., Sanna, A., *et al.* 2012, *A&A*, 539, A79
- Sakai, N., Nagayama, T., Nakanishi, H., *et al.* 2020, *PASJ*, 72(4), 53

- Sakai, N., Reid, M. J., Menten, K. M., Brunthaler, A., & Dame, T. M. 2019, *ApJ*, 876(1), 30
- Sandstrom, K. M., Peek, J. E. G., Bower, G. C., Bolatto, A. D., & Plambeck, R. L. 2007, *ApJ*, 667(2), 1161
- Sanna, A., Moscadelli, L., Cesaroni, R., *et al.* 2010, *A&A*, 517, A78
- Sanna, A., Moscadelli, L., Surcis, G., *et al.* 2017, *A&A*, 603, A94
- Sanna, A., Surcis, G., Moscadelli, L., *et al.* 2015, *A&A*, 583, L3
- Schönrich, R. 2012, *MNRAS*, 427(1), 274
- Skowron, D. M., Skowron, J., Mróz, P., *et al.* 2019, *Science*, 365(6452), 478
- VERA Collaboration, Hirota, T., Nagayama, T., Honma, M., *et al.* 2020, *PASJ*, 72(4), 50
- Weaver, H. 1974, in F. J. Kerr & S. C. Simonson (eds.), *Galactic Radio Astronomy*, 60, 573
- Weidner, C. & Vink, J. S. 2010, *A&A*, 524, A98
- Wu, Y. W., Reid, M. J., Sakai, N., *et al.* 2019, *ApJ*, 874(1), 94
- Xu, Y., Bian, S. B., Reid, M. J., *et al.* 2021, *ApJS*, 253(1), 1
- Xu, Y., Hou, L.-G., & Wu, Y.-W. 2018, *Research in Astronomy and Astrophysics*, 18(12), 146